Determination of Typical Flexural Reinforcement Area in Negative Region of Composite Beam

Abdul Qader Melhem, Mohammad Jamil Kayali
Dept. of Structural Eng., Faculty of Civil Engineering, University of Aleppo, Syria
kayali.2020@jmail.com

Received:15/06/2020
Accepted:28/08/2020

ABSTRACT- Continuous steel beams with reinforced concrete slabs on their top are more economical and effective than classic RC beam models (Reinforcement concrete beams). Also, they are favorite in architectural designs due to their less heights, large spans and ideal resistance to deflection. However, they suffer from several undesirable structural defects, such as local buckling or lateral torsional buckling, so it is necessary to conduct more research and studies on their flexural behavior. In this paper, a mathematical model is prepared and suggested to simulates several experimental samples of continuous composite beam sections using the ANSYS 14 program, then comparing the analytical results with numerical experimental curves (load - deflection) to adjust the validity and accuracy of this suggested mathematical model. Typical reinforcement area value and corresponding resisting bending moment were also determined using this mathematical model for several experimental samples. Furthermore, theoretical formulas have been derived to determine the typical reinforcement area and corresponding bending moment of composite section in negative region, and compare the results of these formulas with the analytical results from numerical model and with values proposed by the codes. Finally, several user-friendly design curves were developed to help in computing the typical reinforcement area values for the composite section within the negative area for continuous steel beam of symmetric flanges. Among the most important results reached, is that reinforcement area ratio is not a fixed ratio but rather related to the properties of the steel and composite section and that it is not advisable to use reinforcement quantities greater than the typical value.

Key words: *Composite - Hogging Moment - Continuous - Beams – numerical - modeling.*

المستخلص – الجيزان الفولاذية المستمرة مع بلاطات بيتونية مسلحة على أعلاها هي أكثر اقتصادية وفعالية من الجيزان البيتونية ذات النمط التقليدي (جيزان البيتون المسلح)، أضف إلى كونها مفضلة فيى التصاميم المعمارية بسبب ارتفاعاتها الاقل ومجازاتها الكبيرة و مقاومتها الجيدة للسهوم، إلا أنها تعاني من عدة عيوب إنشائية غير مرغوبة كالتحنيب الموضعي أو التحنيب الجانبي لذا لا بد من إجراء العديد من الأبحاث والدراسات على سلوكها الانعطافي. تم وفق هذا البحث إعداد نموذج رياضي يحاكي عدة عينات تجريبية لمقطع جائز مركب مستمر بالإعتماد على برنامج (ANSYS 14) ثم مقارنة منحنيات (الحولة – السهم) لضبط صحة و دقة هذا النموذج العددي كما تم تحديد قيمة التسليح المثالية و العزم المقاوم الموافق لها بالإعتماد على هذا النموذج الرياضي لعدة عينات تجريبية أيضاً تم إشتقاق مجموعة من العلاقات النظرية التي تحدد قيمة التسليح المثالية و العزم المقاوم الموافق لها للمقطع المركب ضمن المنطقة السالبة و مقارنة نتائج هذه العلاقات مع النتائج التحليلية للنموذج العددي و بعض القيم المقترحة من قبل الكودات أخيراً تم وضع عدة منحنيات تصميمية سهلة الإستخدام تساعد في الوصول لقيم التسليح المثالية للمقطع المركب ضمن المنطقة السالبة لجائز فولاذي مستمر متناظر. ومن أهم النتائج التي تم التوصل إليها بأن نسبة مساحة التسليح ليست نسبة ثابتة إنما تتعلق بخصائص المقطع المركب والفولاذي وأنه ليس من المجدي وضع كميات تسليح أكبر من القيمة النموذجية.

Introduction

Composite continuous steel beams [1-2] are designed in positive moment regions on the basis that they are composite sections consisting of steel beam and compression part of the concrete slab, its width is called the effective width (be), whose value is determined according to either specifications (AISC) [3] or (AASHTO) [4].

In negative moment regions, the reinforced concrete slab is often neglected [5-6]. This longitudinal reinforcing bars that extend within the slab parallel to the beam and located within the effective width are an important part of the composite section within negative regions, Figure1. Therefore, this reinforcement plays an important role in determining the flexural behavior of the section and may control the potential collapse mode [7] ,so it is necessary to search for the typical and economic value of this reinforcement.

American specifications (AASHTO) [4] mentioned some general recommendations regarding this reinforcement, the reinforcing area of the composite section within the negative moment regions of continuous beam is not less than (A_{sr} > 0.01 * A_g) where two thirds of this area (2/3 * A_{sr}) is placed within the effective width area and the rest outside the effective width area.

Where (A_g) is the area of the cross section of concrete slab between axes of steel beams, see Figure 2.

The importance of research and its objectives:

One of the most important objectives of this paper is to investigate the typical value of the longitudinal reinforcement area (A_{sr}) required for the composite section within the negative region. The results from analytical computer modeling and theoretical derived set of formulas and equations, will be compared with some relevant research done by other researchers.

Several user-friendly design curves will be drawn, to determined typical value of (A_{sr}). On the other hand, since most of the specifications and codes provide general ratios for this reinforcement ignoring properties of the composite section, this paper will find these relations.

The typical reinforcement area:

The typical area is the reinforcement area that causes the strain at the outer fibers, top and bottom, of the composite section to reach their maximum values at the same time. That ensures optimum investment of the section components by obtaining the least required quantities while achieving a balance in the strain behavior of the composite section and finally controlling the expected collapse pattern. That is within several stages, Figure 3. Therefore, the reinforcement area here, can be called the typical, economic or balance area.

Elastic Flexural Behavior of Composite Sections: The First Method:

Properties of composite section are calculated after converting it into a homogeneous section. Stresses are calculated and compared with the allowable ones according to the following relationships [3]:

$$\sigma_{s.bar} = \frac{M.\,y_{top}}{I_{tr}} \le F_{b,bar}$$
$$\sigma'_{s.sec} = \frac{M.\,y_{bot}}{I_{tr}} \le F_b \qquad (1)$$

Where: $\sigma_{s.bar}$: tensile stress in the top reinforcing bars, within concrete slab. M: external bending moment. y_{top}: distance from tension bars to the neutral axis. I_{tr}: moment of inertia of composite section in the negative region. $\sigma'_{s,sec}$: compression stress in steel section. y_{bot}: distance from compression fiber to the neutral axis. F_b: allowable stress in steel fibers, compact or non-compact [3]. $F_{b,bar}$: allowable tension stress in steel bars.

The second method:

This method is based on the calculation of resisting moment of the composite section and comparing it with the applied external moment. The most important step in this method is determination location of the neutral axis according to the design method used [8].

Mathematical model:

The mathematical model studied in this paper is a composite beam of a steel symmetrical section with a concrete slab installed on the its top. The slab is fixed on top of steel beam via shear connectors that provide full composite action. The beam consists of one span with two cantilevers on both ends of the span. This beam is exposed to two concentrated increasing loads at the ends of cantilevers, increased until the collapse, Figure 6. The results of analytical modeling are compared with experimental model [9] to ensure the accuracy of the mathematical model.

Three experimental models were mathematically modeled in this paper (B_1, B_2 and B_3), They differ in steel section and in amount of longitudinal reinforcement placed within the concrete slab, A_{sr}, Table 1.

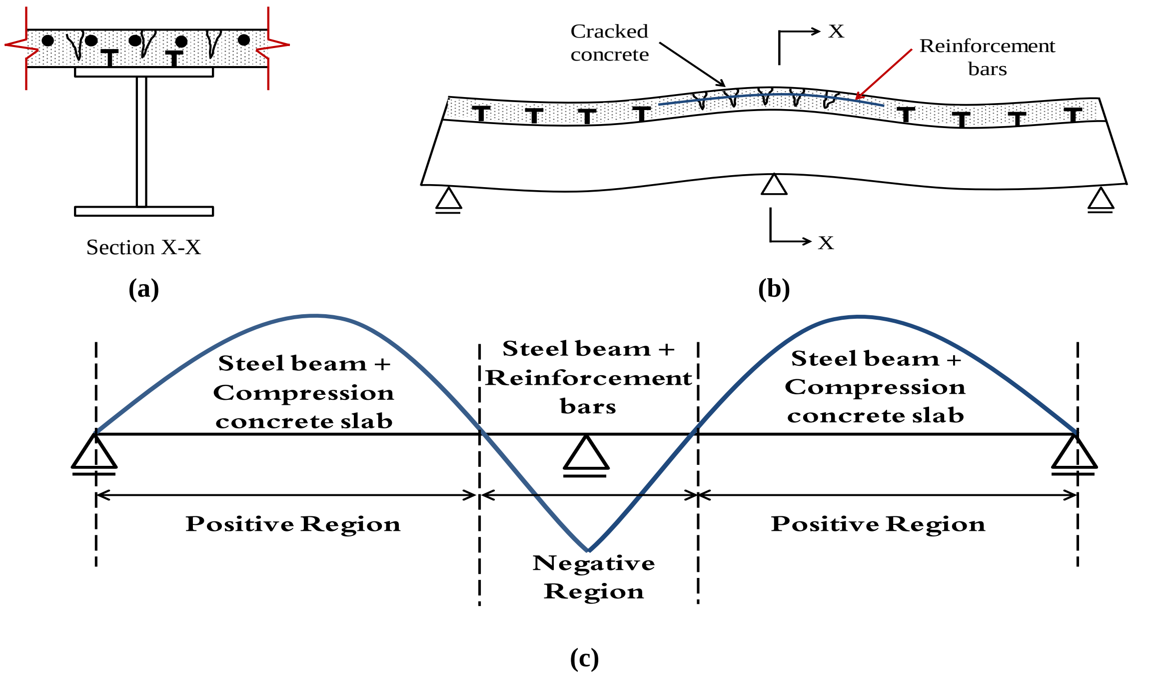

Figure 1: Composite continuous beam (a) cross section within negative region (b) Cracked concrete at negative region (c) Components of the Composite section in both the positive and negative regions

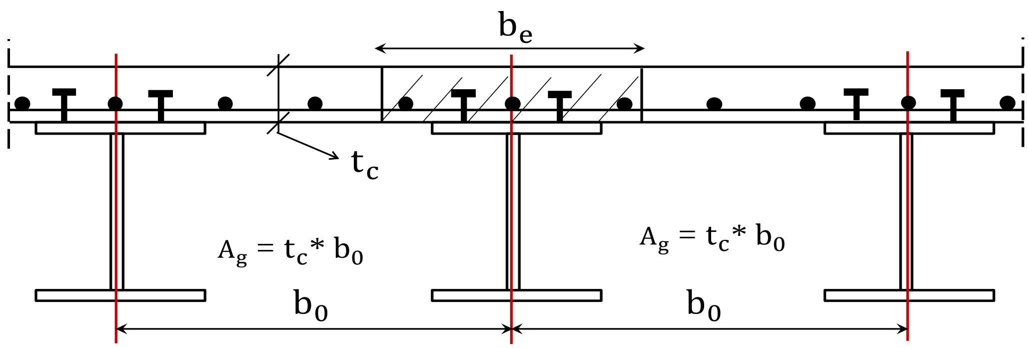

Figure 2: Effective width of the concrete slab that works with the steel profile.

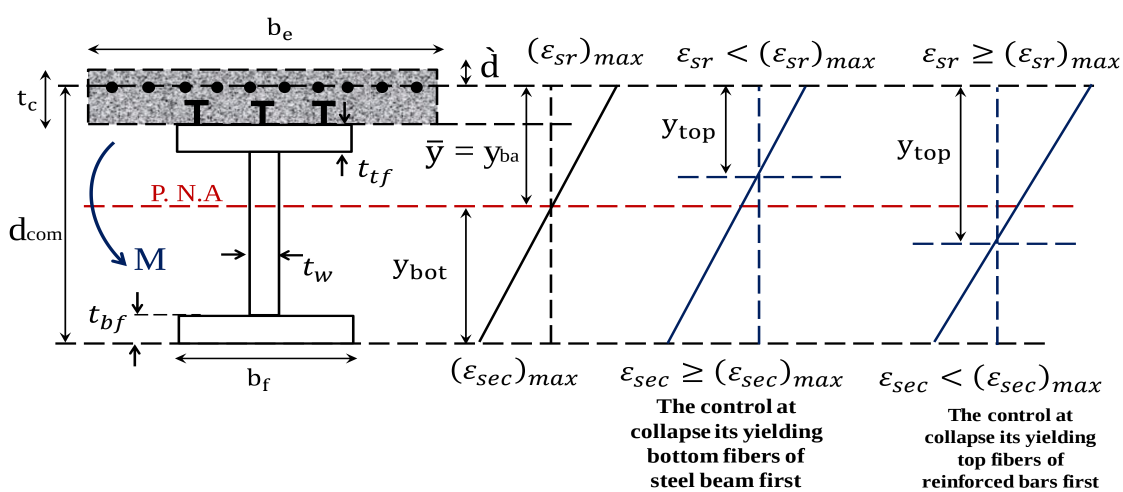

Figure 3: Potential collapse states of the composite section fibers within the negative region.

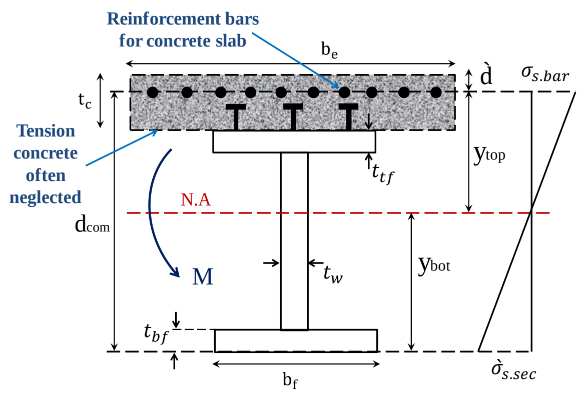

Figure 4: Cross section in the negative region

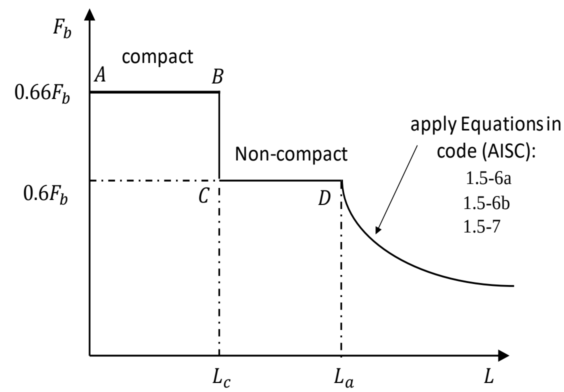

Figure 5: Allowable steel stresses (AISC) [3]

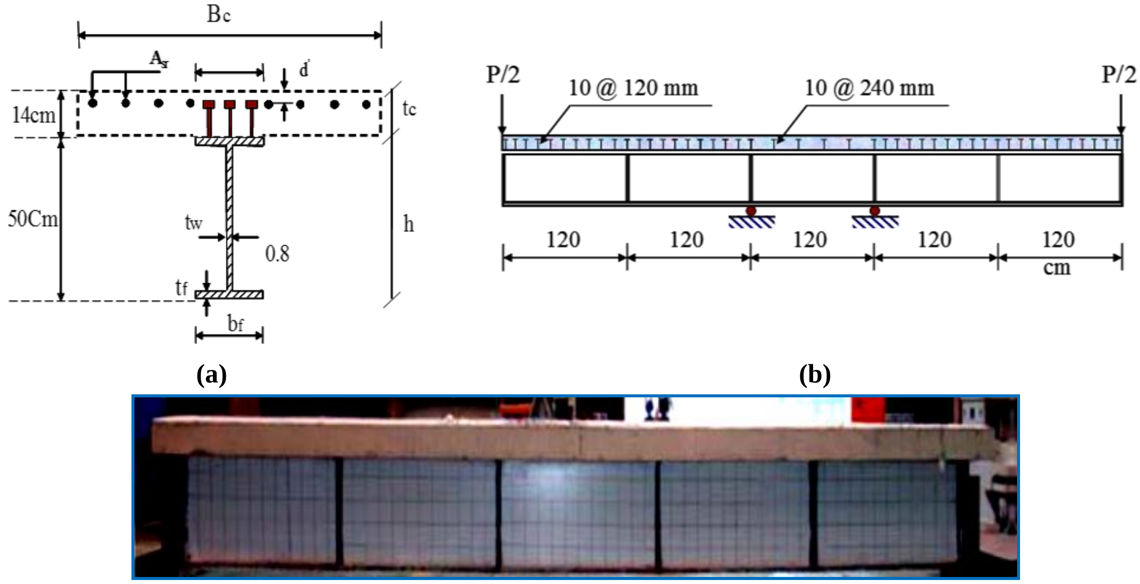

(c)

Figure 6: The studying composite beam model (a) cross section (b) Longitudinal section shows loads sites (c) The real prototype sample [9].

Table 1: Dimensions Of Studied Beam Sections (Mm)

	Ø	%ρ	t_w	h	t_f	B_f	t_c	B_C
B_1	13	1.14	8	500	16	200	140	1000
B_2	16	1.72	8	500	12	220	140	1000
B_3	19	2.43	8	500	10	240	140	1000

Table 2: Material Properties In (Mpa)

	f_y	f_{yr}	f'_c
Steel Section	320	650	
Reinforcement bars	400	520	
Concrete Slab			30.24

Method of Preparing the Mathematical Model (Modeling):

together using the (overlap) feature and connecting elements (Targe170-Conta174) in order to secure full composite action. Transverse stiffener elements on the body and at the support also modeled, taking into account the modeling of half beam to ease and speed the analysis process, Figure 7.

Elements Used in the Mathematical Model (Element Type):

To construct the numerical model, three types of elements were used. Elements of (solid185), (solid65) and (link180) shown in Figure 8 were used to model the steel section, concrete slab and longitudinal reinforcing bars within the concrete slab respectively.

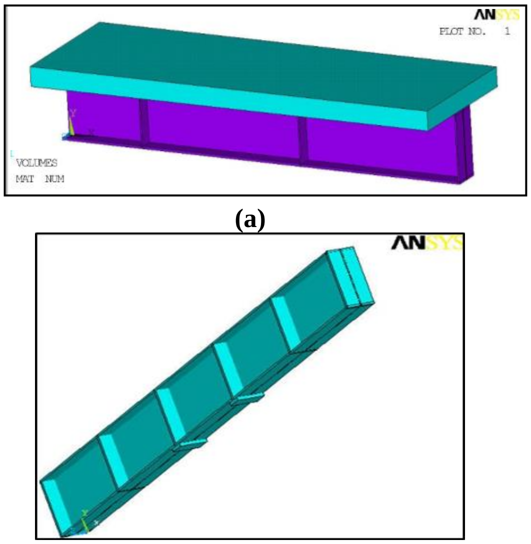

(a)

(b)

Figure 7: Composite beam during the modeling process (a) composite beam (b) steel beam only.

Definition of Material Properties

Table 3 shows the properties of the materials used in preparing the mathematical model. Sargin relationship [11] were used to represent the behavior of the concrete slab. Figures 9, 10 and 11 show behavior curves for each of the steel beam, reinforcing bars, and concrete slab respectively.

The Division of Finite Elements (Meshing):

The dividing process has an important role in the analysis [12], Figure 12 shows the division process of the concrete slab and the steel beam.

Comparing the Experimental Results with Analytical Results of The Mathematical Model:

Curves (Load - Deflection):

Figure 13 shows a comparison between (load – deflection) experimental curves and analytical curves at the free end of the three experimental samples (B_1 - B_2 - B_3) shown. It is seen from these curves that the maximum value of the analytic load in the first beam (B_1) is less than the experimental load (5.47%), while in the second beam (B_2) the relative difference was (9.09%), and in the third beam (B_3) the ratio was (7.2%), Table 4. This means that the mathematical model has an acceptable tolerance in comparison with the experimental samples. This difference may be attributed to the various circumstances occurred during the test.

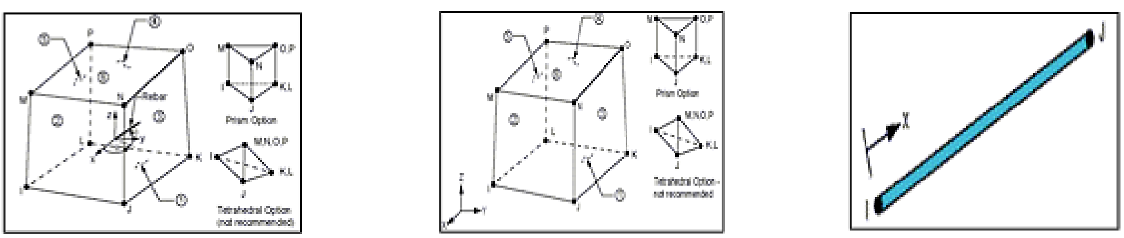

(a) (b) (c)

Figure 8: Types of elements used in the modeling process (a) Volumetric element Solid 65 (b) Volumetric element Solid 185 (c) linear element Link 180

TABLE 3: THE PROPERTIES OF MATERIALS USED IN ANSYS MODELING

	E_x (MPa)	PRXY	f_y (MPa)	$\acute{f}_c$ (MPa)
Steel beam	200000	0.3	320	-
Reinforcing bars	200000	0.3	400	-
Concrete slab	34270	0.2	-	30.24

Theoretical study to determine the typical reinforcement area:

Location of the plastic neutral axis (PNA):

If the following inequality 2 is realized, the PNA is located in the top flange, otherwise it is located in the web.

$$\bar{y} = \bar{\alpha} * d_{com} \le t_{tf} + d_{slab}$$

$$\bar{y} = \bar{\alpha} * d_{com} \ge d_{slab}$$

$$d_{slab} = t_c - \grave{d} \quad , \quad d_{com} = h_s + d_{slab} \qquad (2)$$

$$\bar{\alpha} = \frac{1}{1+\bar{m}} \quad , \quad \bar{m} = {}^{\varepsilon_{sec}}/_{\varepsilon_{sr}} \qquad (3)$$

$$\varepsilon_{sr} = \frac{f_{yr}}{E_s} \quad , \quad \varepsilon_{sec} = \frac{f_{y-sec}}{E_s}$$

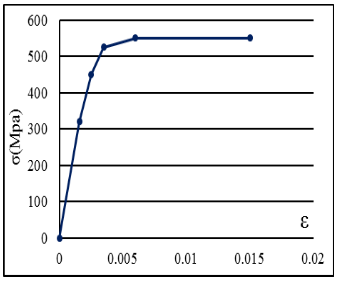

Figure 9: Curve (Stress-Strain) of steel section.

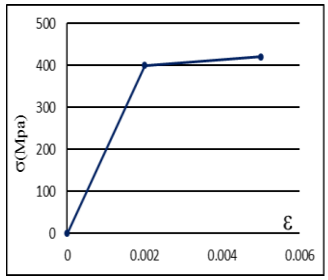

Figure 10: Curve (Stress-Strain) of steel bars.

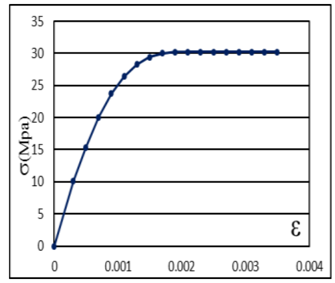

Figure 11: Curve (stress - strain) of the concrete slab.

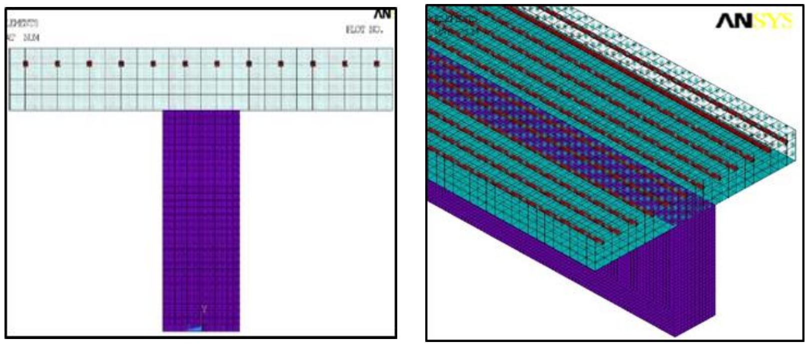
Figure 12: Part of the composite beam after the division process with its cross section.

TABLE 4: DIFFERENCE IN THE MAXIMUM LOAD VALUE BETWEEN THE EXPERIMENTAL BEAMS (EXP.) AND ANALYTICAL BEAMS (ANSYS.)

	B1-Ansys	B1-exp.	B2-Ansys	B2-exp.	B3- Ansys	B3-exp.
Maximum load (KN)	760	804	650	715	580	625
Relative difference in load values	**-5.47%**		**-9.09%**		**-7.20%**	

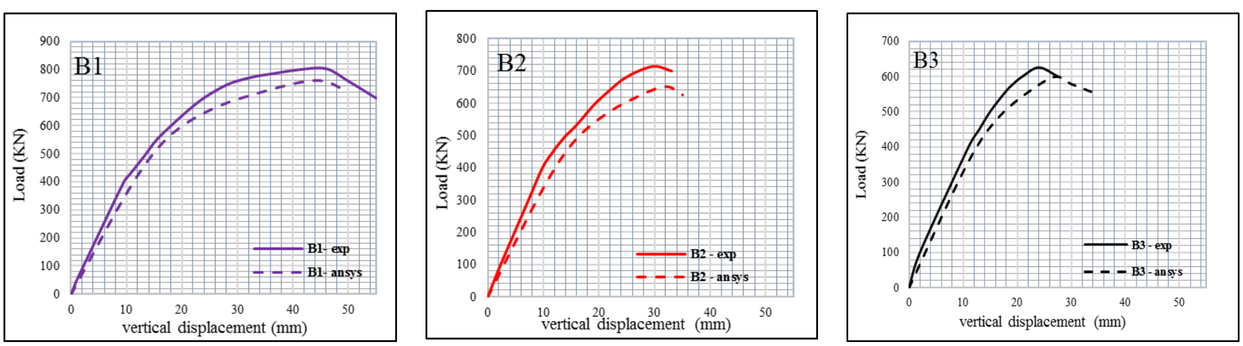

Figure 13: Comparison of experimental and analytical (load-deflection) curves.

The First Case: Neutral Axis Is in the Web:
Figure 14 shows the details of this case where the required reinforcing area for this case is calculated from equations 4, which can be called the balanced or typical area:

$$T_{sr} = A_{sr} * f_{yr} \quad , \quad T_{tf} = f_{y-sec} * t_{tf} * b_{tf}$$
$$T_w = f_{y-sec} * t_w * (\bar{y} + \grave{d} - t_c - t_{tf})$$
$$C_w = f_{y-sec} * t_w * (d_{com} - \bar{y} - t_{bf})$$
$$C_{bf} = f_{y-sec} * t_{bf} * b_{bf} \qquad (4)$$
$$\bar{A}_{sr} = \frac{C_{bf} + C_w - T_{tf} - T_w}{f_{yr}}$$

The ultimate bending moment is calculated from equation 5:

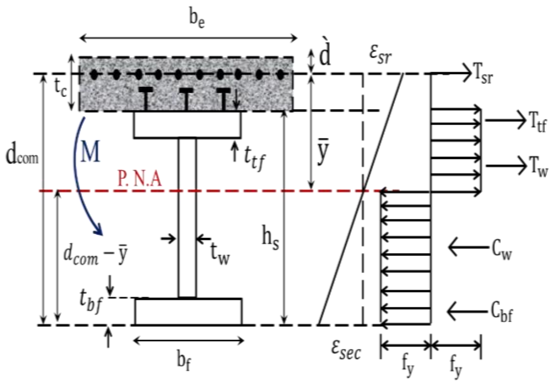

Figure 14: Neutral axis is in the web of steel beam

$$\bar{M} = T_{sr} * \bar{y} + T_{tf} * \left(\bar{y} + \grave{d} - t_c - \frac{t_{tf}}{2}\right) + \frac{T_w}{2} * (\bar{y} + \grave{d} - t_c - t_{tf}) + C_{bf} * \left(d_{com} - \bar{y} - \frac{t_{bf}}{2}\right) + \frac{C_w}{2} * (d_{com} - \bar{y} - t_{bf}) \quad (5)$$

The second case: neutral axis is in top flange:

Figure 15 shows the details of this case and the required reinforcing area for this case is calculated from equations 6, which can be called the balanced or typical area:

$$T_{tf} = f_{y-sec} * b_{tf} * (\bar{y} + \grave{d} - t_c)$$
$$T_{sr} = A_{sr} * f_{yr}$$
$$C_w = f_{y-sec} * d_w * t_w$$
$$C_{bf} = f_{y-sec} * t_{bf} * b_{bf}$$
$$C_{tf} = f_{y-sec} * b_{tf} * (d_{com} - \bar{y} - t_{bf} - d_w)$$
$$\bar{A}_{sr} = \frac{C_{tf} + C_w + C_{bf} - T_{tf}}{f_{yr}} \quad (6)$$

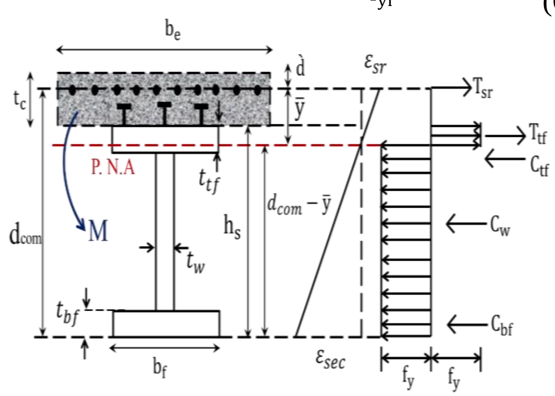

Figure 15: The neutral axis located within the top flange of the steel beam

The ultimate moment is calculated from equation 7:

$$\bar{M} = T_{sr} * \bar{y} + \frac{T_{tf}}{2} * (\bar{y} + \grave{d} - t_c) + \frac{C_{tf}}{2} * (d_{com} - \bar{y} - t_{bf} - d_w) + C_{bf} * \left(d_{com} - \bar{y} - \frac{t_{bf}}{2}\right) + C_w * \left(d_{com} - \bar{y} - t_{bf} - \frac{d_w}{2}\right) \quad (7)$$

Comparing the Results of Theoretical Formulas Versus Analytical Results of the Mathematical Model:

According to the theoretical formulas derived previously, the typical reinforcing values are equal to the experimental values (B_1, B_2 and B_3). The value is (A_{sr} = 213.33 mm^2), where the neutral axis is in the web. The ultimate bending moment corresponding to this reinforcing was variable from one sample to another, Table 5.

The analytical mathematical model by ANSYS14 program, gives values close to the theoretical values, Figure 16. The pattern of division plays an important role in narrowing these differences between theoretical and analytical values, where the convergence between them is noticeable. This ensures the correctness of both the mathematical model and theoretical formulas.

Comparing among the theoretical formula values and experimental values and code values:

The reinforcing areas in the experimental samples (B_1, B_2 and B_3) are greater than the theoretical reinforcing values, Table 6, which predicts collapse either by yielding of bottom fiber of the steel section or local buckling of the compressed bottom flange, this is what the researcher has indicated [9]. In the experimental work, all the collapse mechanisms were followed the aforementioned pattern, no yielding of the reinforcing bars was observed.

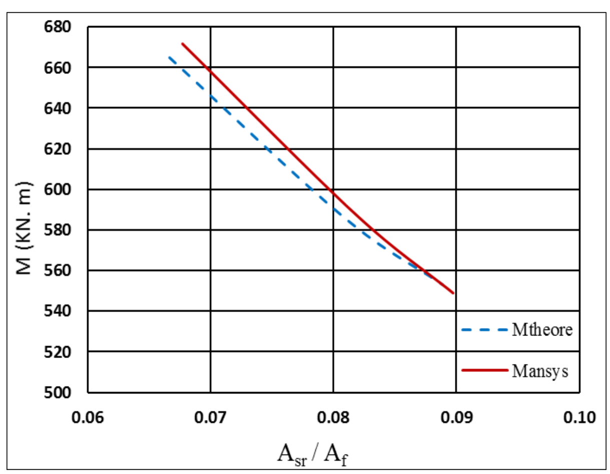

Figure 16: A comparison between theoretical and analytical values of the typical reinforcing area with the corresponding moment.

TABLE 5: VALUES OF THEORETICAL AND ANALYTICAL TYPICAL REINFORCING AREA WITH THE CORRESPONDING MOMENT.

Sample	B1	B2	B3
Flange Area (mm^2)	3200	2640	2400
Theoretical reinforcing area (mm^2)	213.33	213.33	213.33
Analytical reinforcing area (mm^2)	216.72	215.84	215.43
Theoretical ultimate moment (KN.m.)	664.95	586.43	552.93
Analytical ultimate moment (KN.m.)	671.92	588.13	548.87

The relative difference in the reinforcement area values reached (93%) in the sample (B_3), which had largest reinforcing area and smallest flanges, while the difference in moment was (26%). In the sample (B_1) with the smallest reinforcing area and the largest flanges, the relative difference in the reinforcement was (86%), while in the moment values (31%), the sample (B_3) has twice as much as the reinforcing area of the sample (B_1) and the smallest flanges, but the difference in moment did not double.

TABLE 6: VALUES OF EXPERIMENTAL AND THEORETICAL REINFORCING AREA WITH THE CORRESPONDING MOMENT

The Sample	B1	B2	B3
Concrete slab area (mm^2)	140000	140000	140000
Flanges area (mm^2)	3200	2640	2400
Height of steel section (mm)	500	500	500
Experimental reinforcing area (mm^2)	1596	2408	3402
Theoretical reinforcing area (mm^2)	213.33	213.33	213.33
Experimental moment (KN.m)	964.8	858	750
Theoretical moment (KN.m)	664.95	586.43	552.93
Relative difference in reinforcing values	%86.63	%91.14	%93.73
Relative difference in moments values	%31.1	%31.65	%26.28

This indicates that there is a large amount of reinforcement wasted without a role (area above typical), and that the flanges played a role in determining the bending resistance, Figure 17.

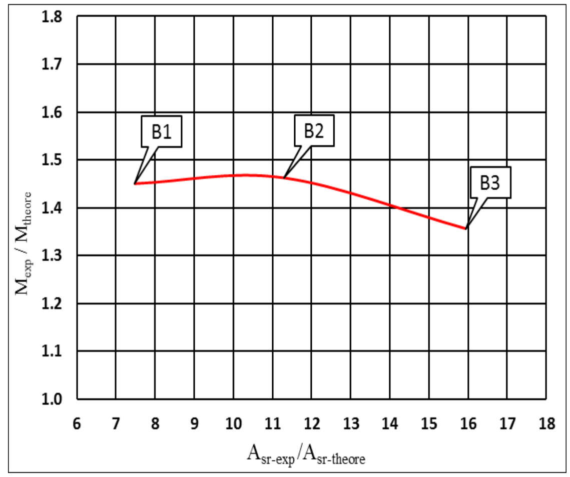

Figure 17: The relationship between the ratio of experimental to theoretical reinforcing areas with the ratio of corresponding moments

TABLE 7: THE VALUES OF THEORETICAL REINFORCING AREAS AND ACCORDING TO (AASHTO) WITH THE CORRESPONDING MOMENTS

The Sample	B1	B2	B3
Concrete slab area (mm^2)	140000	140000	140000
Flanges area (mm^2)	3200	2640	2400
Height of steel section (mm)	500	500	500
Required reinforcing area according to AASHTO (mm2)	933.33	933.33	933.33
Theoretical reinforcing area (mm^2)	213.33	213.33	213.33
Ultimate moment according to the reinforcing area by AASHTO (KN.m)	752.85	674.33	640.83
Theoretical ultimate moment (KN.m)	664.95	586.43	552.93
Relative difference in reinforcing values	%77.14	%77.14	%77.14
Relative difference in moments values	%11.68	%13	%13.72

The required reinforcing area for these three models (B_1, B_2 and B_3) was calculated according to (AASHTO) [4] ratio, which is not less than ($0.0067 * A_g$). It is greater than the theoretical typical reinforcing areas. It is nearly four times greater, while the difference in the ultimate bending does not exceed (14%), Table 7.

This is due to that AASHTO gives same area for the three samples, its area relates only to the concrete slab area without regard to the specifications of the steel section, which is one of the basic parts of the composite section within the negative region.

Designing curves to determine the typical reinforcing area:

These curves are designed in the simplest possible form to calculate the typical reinforcing area required for the composite section within the negative region. They are specific to the symmetrical steel sections in the form of (I-steel section). Working steps can be explained:

Calculate the following percentage:

$$\bar{m} = \frac{f_{y-sec}}{f_{yr}} \leq 1$$

Calculate the following percentage:

$$\bar{\alpha} = \frac{1}{1+\bar{m}}$$

Calculate the effective depth of the concrete slab:

$$d_{slab} = t_c - \grave{d}$$

Calculate the total height of the composite section:

$$d_{com} = h_s + d_{slab}$$

Calculates the location of the plastic neutral axis:

$$\bar{y} = \bar{\alpha} * d_{com}$$

Calculates this following distance:

$$Z = \bar{y} - d_{slab} \geq 0$$

If ($Z < 0$), the neutral axis is in the tension concrete slab and this designing case is rejected. The following percentage is calculated to determine the location of the neutral axis.

- If $Z/t_f < 1$, neutral axis is in the top flange.
- If $Z/t_f \geq 1$, neutral axis is in the web.

If the neutral axis is in the web, the curves shown in Figure 18 are used to determine the typical required reinforcing area according to the following values:

$$\left(\frac{h_s}{d_{slab}}\right) \quad , \quad A = \bar{m} * t_w * d_{slab}$$

If the neutral axis is in the top flange, the curves shown in Figure 19 are used to determine the typical reinforcing area required according to the following values:

$$K = A_f + \frac{A_w}{2} - b_f * Z$$

$$\bar{m} = \frac{f_{y-sec}}{f_{yr}} \leq 1$$

where: A_f: flange area, A_w: web area, b_f: flange width

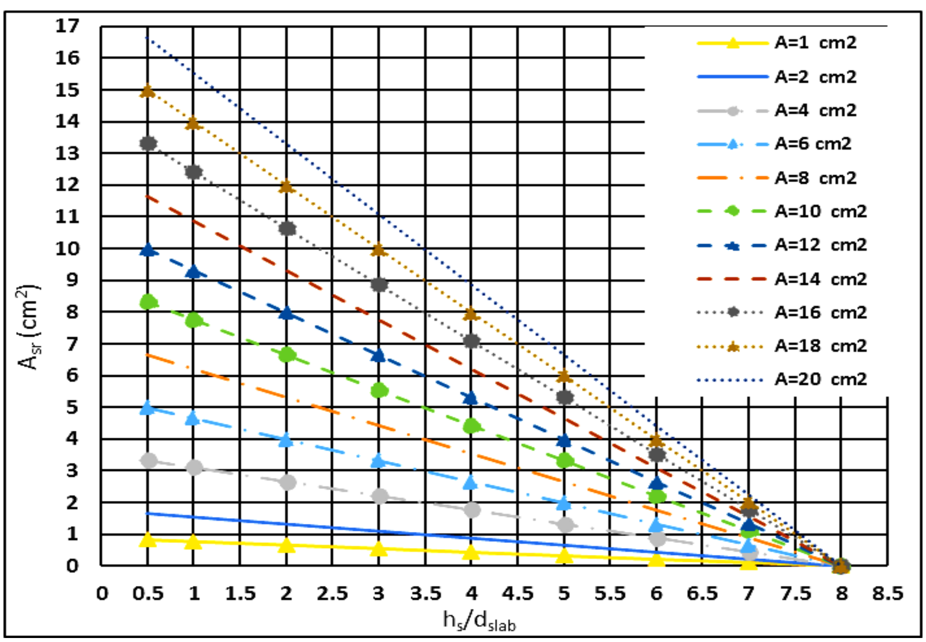

Figure 18: Design curves to calculate the typical reinforcing area: neutral axis is in the web where:

$$\bar{m} = 0.8 \quad - \quad A = \bar{m} * t_w * d_{slab} \quad - \quad \frac{Z}{t_f} \geq 1$$

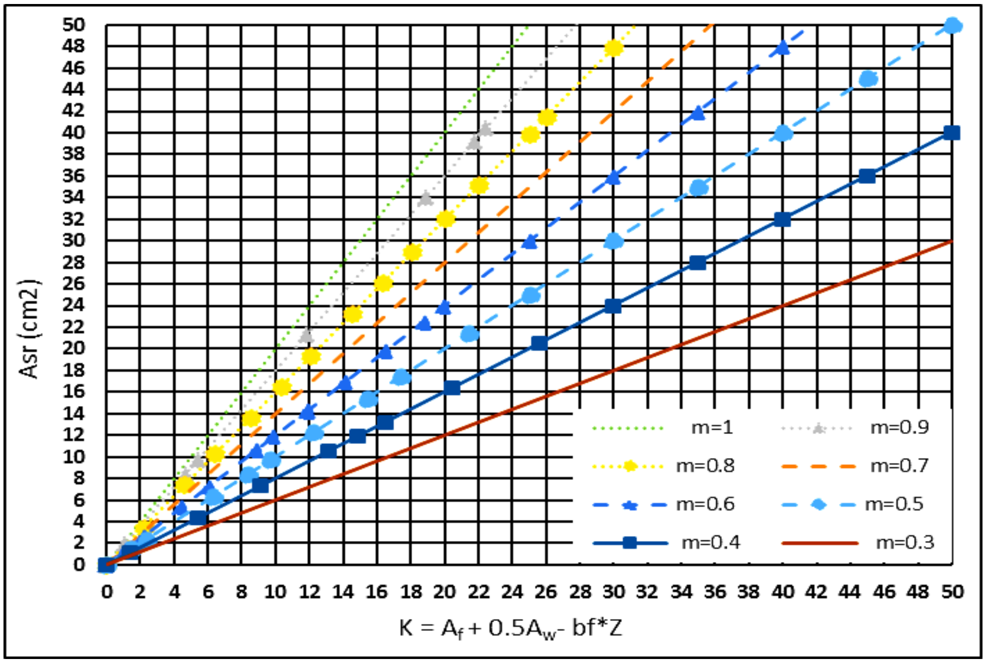

Figure 19: Design curves to calculate the typical reinforcing area: neutral axis is in the top flange where:

$$\frac{\mathbf{Z}}{\mathbf{t_f}} < \mathbf{1}$$

RESULTS DISCUSSION

Based on the results of the study, the following conclusions can be obtained:

i. The required reinforcement area for the composite section in the negative region is not only related to the characteristics of the concrete slab (as presented by several standards), but also related the characteristics of the steel and composite sections as indicated by the output curves, Figure 18 and 19.

ii. The flange area of steel section has a greater role in determining the flexural capacity of the composite section than the reinforcing bars, especially when reinforcing bars exceeds the typical value.

iii. The value of ($\overline{A_{sr}}$) may be adopted as an indicator of the section behavior and the expected pattern of failure, when the composite section contains a reinforcing area greater than the typical value. The failure indicator is yielding the bottom fibers of steel section or the local buckling of bottom flange.

iv. However, when the composite section contains a reinforcing area smaller than the typical value, the indicator of failure will be either the yielding of the reinforcing bars or yielding of the top fibers of steel section

v. It is not useful to place an amount of reinforcement area greater than the typical amount in the composite section within the negative region to raise the bending moment. That increment in bending moment will not justify the increase in the amount of reinforcement, Figure 17

vi. The theoretical relationships derived in this paper to calculate the typical value of reinforcing area in the negative region of the composite section were found in the simplest possible way and give acceptable accuracy compared with the results from analytical model (FEM) as shown in Figure 16. It can be also used for symmetrical and asymmetric steel sections.

vii. In symmetrical sections, the typical reinforcement area has nothing to do with the change of the cross section of flanges, when the neutral axis is located within the web.

viii. When the neutral axis is located within the top steel flange of the composite section, the characteristics of both symmetrical flanges and web play an important role in determining value of the typical reinforcing area.

ix. The required reinforcing area of the composite section within the negative region is not a fixed value or ratio, but rather related to the specifications of the composite section.

x. The numerical modeling showed good efficiency in simulating the experimental models as shown in Curves 13, thus can be useful in saving time and money.

xi. It was found from the analytical and theoretical results of the three experimental samples that the value of ($\overline{A}_{sr}$) has not been changed, it was constant for the three samples. Because the ratio (h_s/d_{slab}) is constant, as well as the properties of the used steel ($\overline{m} = \frac{f_{y-sec}}{f_{yr}}$), while the value of the ultimate moment corresponding to this reinforcement is variable from one sample to another, despite of (h_s) and ($\overline{A}_{sr}$) being constant, but the flange areas are variable. This indicates that the flanges have an important role in determining the bending capacity of the composite section.

xii. It is recommended to expand the previous designing curves (Figure 18 and 19) to become more general and comprehensive by including more steel sections, taking into account the effect of local buckling of the bottom compression flange.

CONCLUSIONS

The longitudinal reinforcement area (A_{sr}) within the concrete slab in the negative region has an important role in determining how the flexural behavior goes, even if it may be a just secondary reinforcement in the whole slab-beam system. This is due to the weak action of tension concrete slab.

The value of this longitudinal reinforcement is not a fixed percentage related to the properties of the concrete slab only as has been mentioned in some literature, but rather related to the properties of the steel section in addition to the specifications of the composite section. Therefore, composite section properties play a major role in determining the value of the required reinforcing area.

The variation of this reinforcement has shown that it is an indicator of the expected collapse pattern of the composite section. Particularly, when its area exceeds the typical value determined by this study. The main failure pattern can be occurring by local buckling of the bottom compression flange (A_f).

The main controlling factor in structural behavior in negative region is the ratio (A_{sr} /A_f), which represents the close relationship between amount of this reinforcement and specifications of the steel beam, or in general the composite beam.

References

[1] Hamada, S. and Longworth, J. (1976), Ultimate Strength of Continuous Composite Beams, Journal of Structural Division, ASCE, Vol.102, ST7, pp. 1463 – 1478.

[2] By G. Fabbrocino, G. Manfred, and E. Cosenza. (2000), analysis of continuous composite beams including partial interaction and bond, 1288 / journal of structural engineering American Institute of Steel Construction

[3] (AISC 2007), Manual of Steel Construction, New York, NY.

[4] AASHTO LRFD Bridge Design Specifications. (1998), SI units, 2nd ed.

[5] Trong-Chuc Nguyen, Trong-Phuoc Huynh, Nguyen-Trong Ho, Al-Amin Abdun Noor., (2019), Evaluating the Effectiveness of Continuous Composite Beams for Steel-Concrete Bridges and Control Concrete Cracks of the Supports at an Early Age, EDP Sciences, E3S Web of Conferences 97, 03007.

[6] G. Vasdravellis, B. Uy, E.L. Tan, B. Kirkland. (2012), Behaviour and design of composite beams subjected to negative bending and compression, Journal of Constructional Steel Research 79 - 2012 34 – 47

[7] Jing Liu, Fa-xing Ding, Xue-mei Liu, Zhi-wu Yu, Zhe Tan, and Jun-wen Huang. (2019), Flexural Capacity of Steel-Concrete Composite Beams under Hogging Moment, Hindawi Advances in Civil Engineering, Volume, Article ID 3453274, 13 pages.

[8] EUROCODE 4 (1994). Design of composite steel and concrete structures part 2. Composite bridges. DD ENV -2. BSI.

[9] Ryua, H. K, Youn, S. G., Bae, D., and Lee, Y. K. (2006), Bending Capacity of composite Girders with Class 3 Section, Journal of Constructional Steel Research, 62, pp. 847–855.

[10] ANSYS Tutorials, Release 14- Documentation for ANSYS.

[11] M. Sargin (1971), Stress-Strain Relationship for Concrete and the Analysis of Structural Concrete Sections, Study 4, Solid Mechanics Division; University of Waterloo, Waterloo, Canada.

[12] Xiaolin chen and Yijun liu. (2015), Finite element Modeling and simulation with Ansys Workbench, Book by Taylor and Francis group.